

Landslides (2020) 17:517–526  
 DOI 10.1007/s10346-019-01292-7  
 Received: 14 June 2019  
 Accepted: 13 September 2019  
 Published online: 9 November 2019  
 © The Author(s) 2019

Sophia Barth · Marten Geertsema · Alexandre R. Bevington · Alison L. Bird · John J. Clague · Tom Millard · Peter T. Bobrowsky · Andreas Hasler · Hongjiang Liu

## Landslide response to the 27 October 2012 earthquake ( $M_w$ 7.8), southern Haida Gwaii, British Columbia, Canada

**Abstract** In this paper, we examine the influence of the 27 October 2012,  $M_w$  7.8 earthquake on landslide occurrence in the southern half of Haida Gwaii (formerly Queen Charlotte Islands), British Columbia, Canada. Our 1350 km<sup>2</sup> study area is undisturbed, primarily forested terrain that has not experienced road building or timber harvesting. Our inventory of landslide polygons is based on optical airborne and spaceborne images acquired between 2007 and 2018, from which we extracted and mapped 446 individual landslides (an average of 33 landslides per 100 km<sup>2</sup>). The landslide rate in years without major earthquakes averages 19.4 per year, or 1.4/100 km<sup>2</sup>/year, and the annual average area covered by non-seismically triggered landslides is 35 ha/year. The number of landslides identified in imagery closely following the 2012 earthquake, and probably triggered by it, is 244 or an average of about 18 landslides per 100 km<sup>2</sup>. These landslides cover a total area of 461 ha. In the following years—2013–2016 and 2016–2018—the number of landslides fell, respectively, to 26 and 13.5 landslides per year. In non-earthquake years, most landslides happen on south-facing slopes, facing the prevailing winds. In contrast, during or immediately after the earthquake, up to 32% of the landslides occurred on north and northwest-facing slopes. Although we could not find imagery from the day after the earthquake, overview reconnaissance flights 10 and 16 days later showed that most of the landslides were recent, suggesting they were co-seismic.

**Keywords** Landslide · Earthquake · British Columbia · Haida Gwaii

### Introduction

Landslides pose a threat to infrastructure and public safety and can induce large-scale ecological change (Smith et al. 1986; Geertsema and Pojar 2007; Schuster and Highland 2007; Geertsema et al. 2009). Although landslides in British Columbia (BC) have been attributed to climatic factors, such as extreme weather events (Schwab 1983, 1998; Evans and Clague 1994; Septon and Schwab 1995; Guthrie and Evans 2004; Jakob and Lambert 2009), degrading mountain permafrost and glacial debuitressing (Geertsema et al. 2006; Cloutier et al. 2016), and land use (Jakob 2000), there are relatively few reports in BC of regional-scale landslides triggered by earthquakes (notable exceptions include papers by Mathews 1979 and Martin et al. 2002). Yet, co-seismic landslides are common in earthquake-prone areas around the world (Tanyaş et al. 2017), including New Zealand (Vittoz et al. 2001; Wells et al. 2001), China (Yin et al. 2009; Xu et al. 2014), Japan (Wang and Sassa 2006), Nepal (Kargel et al. 2016), California (Keefer 2000), and Alaska (Jibson et al. 2006). An earthquake can directly trigger numerous landslides and, as well, reduce soil and rock strength such that

rainfall initiates instability in the months and years following the earthquake (Lin et al. 2006).

Haida Gwaii, an archipelago located in the northeast Pacific Ocean about 50 km west of mainland BC (Fig. 1), is prone to heavy rainfall, strong earthquakes, and frequent landslides (Banner et al. 2014; Bevington et al. 2017). On 27 October 2012, an  $M_w$  7.8 earthquake, the second largest instrumentally recorded earthquake in Canada, occurred approximately 20 km off the coast of Haida Gwaii at a depth of 23 km (Rosenberger et al. 2013; Bird and Lamontagne 2015). The event was recorded on seismographs across North America and much of the world, and notably on strong motion instruments in Masset, the village of Queen Charlotte where a peak horizontal acceleration of 0.2 g was recorded (Bird and Lamontagne 2015), as well as in Prince Rupert on the adjacent mainland (Fig. 1). The earthquake occurred on an unnamed subduction interface beneath the Queen Charlotte Fault, a boundary between the Pacific and North America plates. The fault slipped over an area of about 120 × 50 km. Thousands of aftershocks followed the event, the largest a  $M_w$  6.3 event on October 28, 2012 (Cassidy et al. 2014) and another of  $M_w$  6.1 on October 29, 2012 (Fig. 1). Low altitude overview flights were conducted 10 and 16 days after the earthquake to document earthquake-induced landslides.

The objective of this paper is to compare rates and characteristics of landslides before and after the 27 October 2012 Haida Gwaii earthquake with pre-event baseline landslide inventory data.

### Study area

Our study area covers 1350 km<sup>2</sup> in Gwaii Haanas National Park Reserve and Haida Heritage Site, which includes the southern part of Moresby Island and numerous adjacent smaller islands (Fig. 1). This part of the archipelago lies entirely within the Queen Charlotte Ranges and is characterized by moderate to high relief with peaks ranging in elevation from 1000 m asl (above sea level) in the north to 400–500 m asl in the south.

The bedrock of the study area comprises Triassic basalts of the Karmutsen Formation intruded by Jurassic granitic plutons that form the higher elevation mountains (Sutherland Brown 1968). Lyell Island, a large island in the northeast corner of our study area, is part of the Tertiary Masset Formation consisting of basalts and rhyolites (Sutherland Brown 1968). Sedimentary rocks of Late Triassic to Cretaceous age occur in the north (Sutherland Brown 1968).

The study area is dominated by coniferous forest; the dominant tree species are western hemlock (*Tsuga heterophylla*), Sitka spruce (*Picea engelmannii*), and at higher elevations mountain hemlock (*Tsuga mertensiana*) (Banner et al. 2014). The highest peaks support herbaceous alpine vegetation. The most common

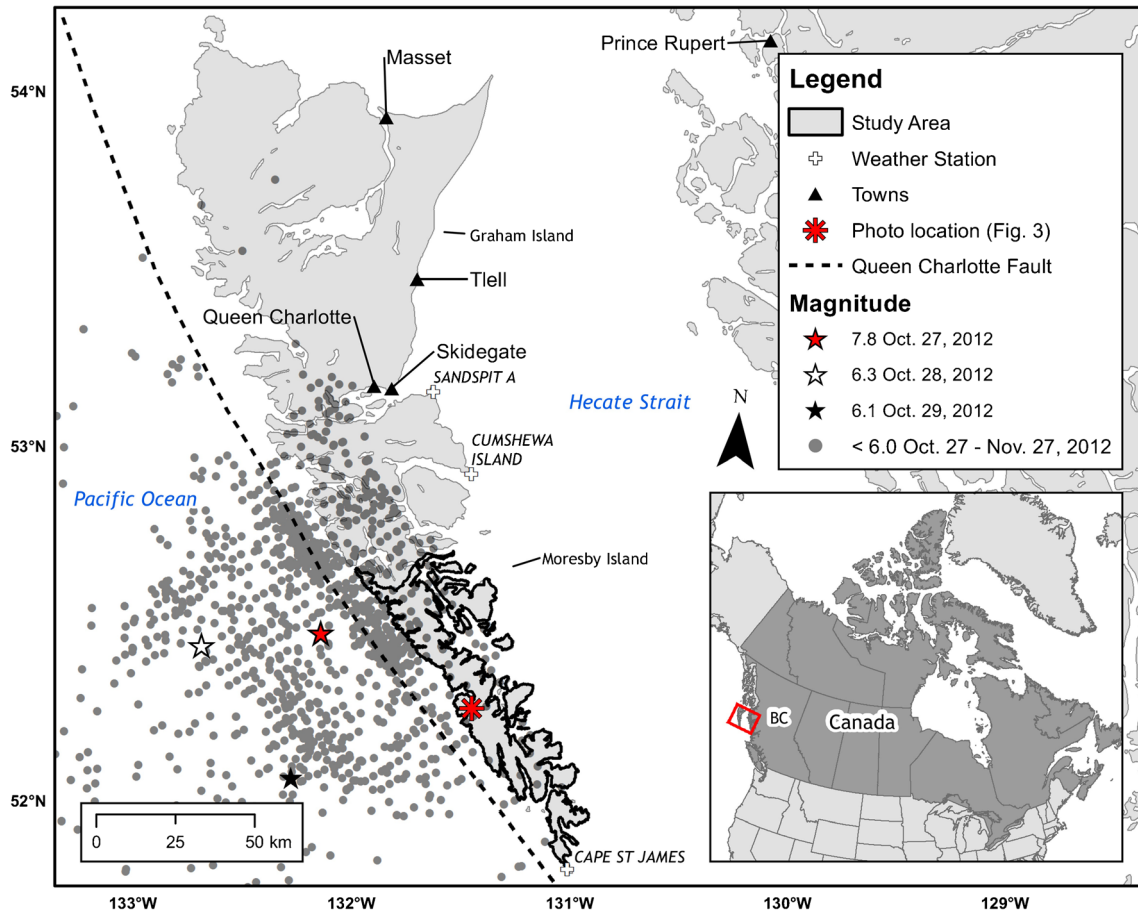


**Fig. 1** Location map of the study area on Haida Gwaii (formerly the Queen Charlotte Islands). Note the Queen Charlotte Fault (dashed line), Environment Canada weather stations, and the main population centres. Earthquakes between 27 October and 27 November 2012 are shown as grey circles if smaller than  $M_w$  6.0 and as stars if larger than  $M_w$  6.0.

soil types are podzols, regosols, and organic soils (Soil Classification Working Group 1998; Banner et al. 2014). Coastal BC, including Haida Gwaii, is known for its upland organic soils (Folisols; Fox and Tarnocai 2011; Banner et al. 2014) that are commonly associated with debris slide initiation zones (Nagle 2000; Blais-Stevens et al. 2016).

Haida Gwaii has a cool temperate, humid to perhumid, oceanic climate (Banner et al. 2014). The temperate climate of the archipelago is influenced by its location in the northeast Pacific Ocean distant from the North American mainland. Temperatures differ little between seasons and rarely fall below 0 °C at low elevations. The dominantly humid climate is, however, strongly influenced by topography. The east coast is much drier than the west coast as it is shielded from humid North Pacific air masses by the Queen Charlotte Ranges, and the higher elevations occasionally support intermittent snow.

Three Environment Canada weather stations are near the study area (Fig. 1). Climate normals derived from the Sandspit A weather station near sea level are based on the years 1981–2010. The mean annual air temperature at Sandspit A is 8.6 °C. The coldest month is January, with an average temperature of 4 °C. August is the warmest month, with temperatures averaging 15.2 °C. Mean annual precipitation (MAP) at the Sandspit A station is 1408 mm, of which

an average of 1371 mm falls as rain. About 78% of the annual precipitation falls between October and April. December is the wettest month, with an average of 196 mm of precipitation. July, the driest month, has an average of 48 mm of rain. Strong prevailing winds, mostly from the southwest, are common on Haida Gwaii. The average wind speed measured at Sandspit A is 19.3 km/h, and the maximum wind gust speed, recorded in 1974, was 164 km/h. Schwab (1983) estimated a 5-year return interval for storms of similar severity to the 1974 event. Bevington et al. (2017) summarized the modelled, mean annual precipitation of Haida Gwaii (Wang et al. 2012) for the period 1961–1990 and showed that a large portion of our study area, some 50–150 km from the Sandspit A station, experiences 3000–5000 mm mean annual precipitation.

#### Seismic history

Haida Gwaii is the most seismically active region in Canada. The dominantly transform Queen Charlotte Fault extends along the full length of the archipelago directly off its western margin (Fig. 1). The relative plate motion, about 50 mm/year (DeMets et al. 1990), is ~15° to 20° oblique to the strike of the fault off Moresby Island. Consequently, there is a component of convergence and compression across this part of the plate boundary,

accommodated by thrust earthquakes; the 2012 earthquake was such an event.

Small and moderate earthquakes around Haida Gwaii were not well recorded before a local seismic network was established in the mid-1980s. Several large earthquakes were recorded by the regional network in the preceding decades, including a magnitude 8.1 event in 1949, the largest instrumentally recorded earthquake in Canada's history (Bostwick 1984). The seismic network installed on the islands and adjacent mainland has revealed high levels of seismicity off the archipelago's west coast, and considerable activity inland, notably on Graham Island and in northern Hecate Strait (Fig. 2).

### Landslide history

Many landslide inventories have been made on Haida Gwaii since the early 1980s (Schwab 1983, 1988; Rood 1984, 1990; Krag et al. 1986; Smith et al. 1986; Gimbarzevsky 1988; Rollerson 1992; Jagielko et al. 2012; Millard et al. 2012). Most of the inventories focused on landscapes subject to forest harvesting, particularly in the north, and were a response to concerns over possible impacts on fish habitats (Poulin 1984; Tschaplinski et al. 2004). In contrast, our study is within parks and protected areas, and concerns only landslides in forested terrain that has not been subject to road building or timber harvesting.

Most of the landslides in past inventories are debris slides, debris flows, and rock slides, in order of decreasing abundance. The largest landslide datasets are those of Rood (1984) and Gimbarzevsky (1988). Rood (1984) mapped more than 1300

landslides in a 350 km<sup>2</sup> area between southern Graham Island and northern Moresby Island using 1:11,000–1:13,000 scale air photos. He estimated a density of 480 landslides per 100 km<sup>2</sup> on steep forested slopes and concluded that landslides were 34 times more frequent on logged slopes than on natural forested ones. Gimbarzevsky (1988) mapped more than 8300 landslides on Haida Gwaii (over almost 10,000 km<sup>2</sup>) using 1:50,000 scale aerial photographs acquired in 1979 and 1980. He found an average of 326 landslides per 100 km<sup>2</sup>. Jagielko et al. (2012) re-analyzed the data of Rood (1984) and Gimbarzevsky (1998), attributing their different landslide rates to the use of different spatial mapping resolutions. Schwab (1983) found 264 mass movements in an area of 160 km<sup>2</sup> in Rennell Sound on the west coast of Graham Island after a major storm in 1978. He calculated a density of 80 landslides per 100 km<sup>2</sup> in forested terrain and about 15 times as many in human-impacted terrain. The areas of all these inventories were affected by timber harvesting and road construction.

### Data and methods

We used photographs taken during aerial reconnaissance flights, high-resolution aerial photos, and satellite images to map landslides.

### Aerial reconnaissance flights

Aerial overview flights (Figs. 3 and 4) were made by helicopter on 7 and 8 November 2012 and by fixed-wing plane on 12 November 2012 (Millard et al. 2012). The 12 November flight covered most of

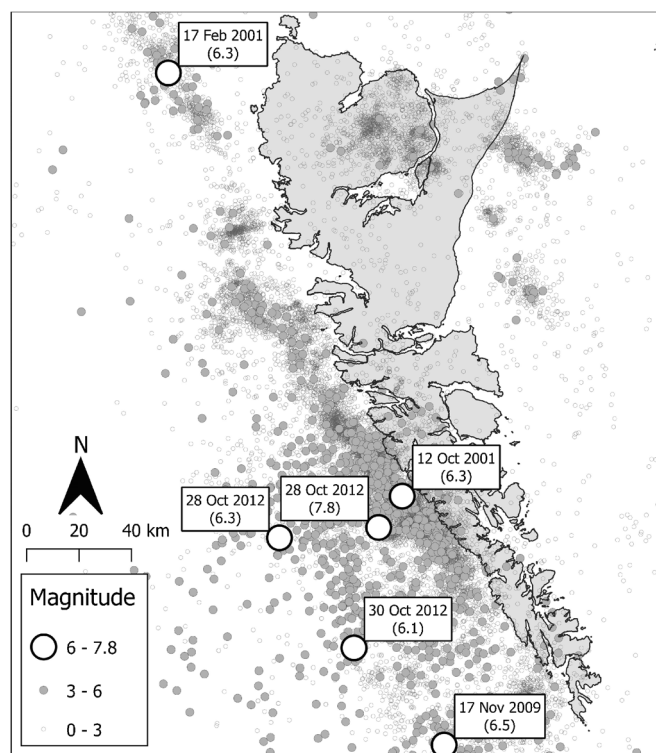


**Fig. 2** Spatial distribution of earthquakes on and near Haida Gwaii. The first earthquake included in this compilation is 1 January 1985 and the last is 10 January 2019. The date and magnitude of earthquakes stronger than  $M_w$  6.0 are shown on the map. Data source: <https://open.canada.ca/data/en/dataset/4cedd37e-0023-41fe-8eff-bea45385e469>

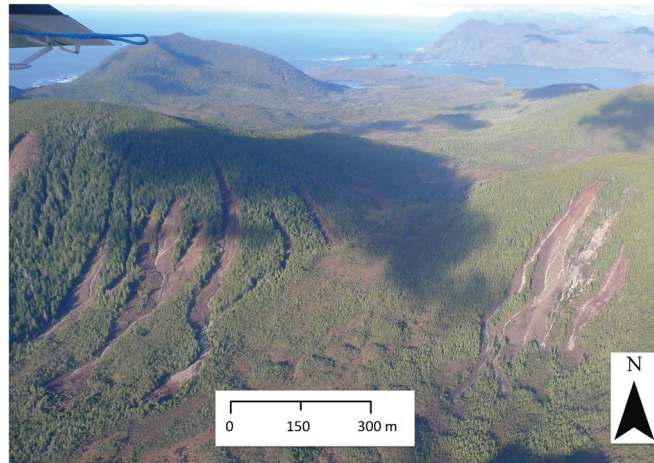


**Fig. 3** Fresh debris slides south of Gowaia Bay, photographed on 12 November 2012, 16 days after the earthquake. Photograph location is shown in Figs. 1 and 4c. Photograph taken by Marten Geertsema. Scale shown pertains to the image foreground

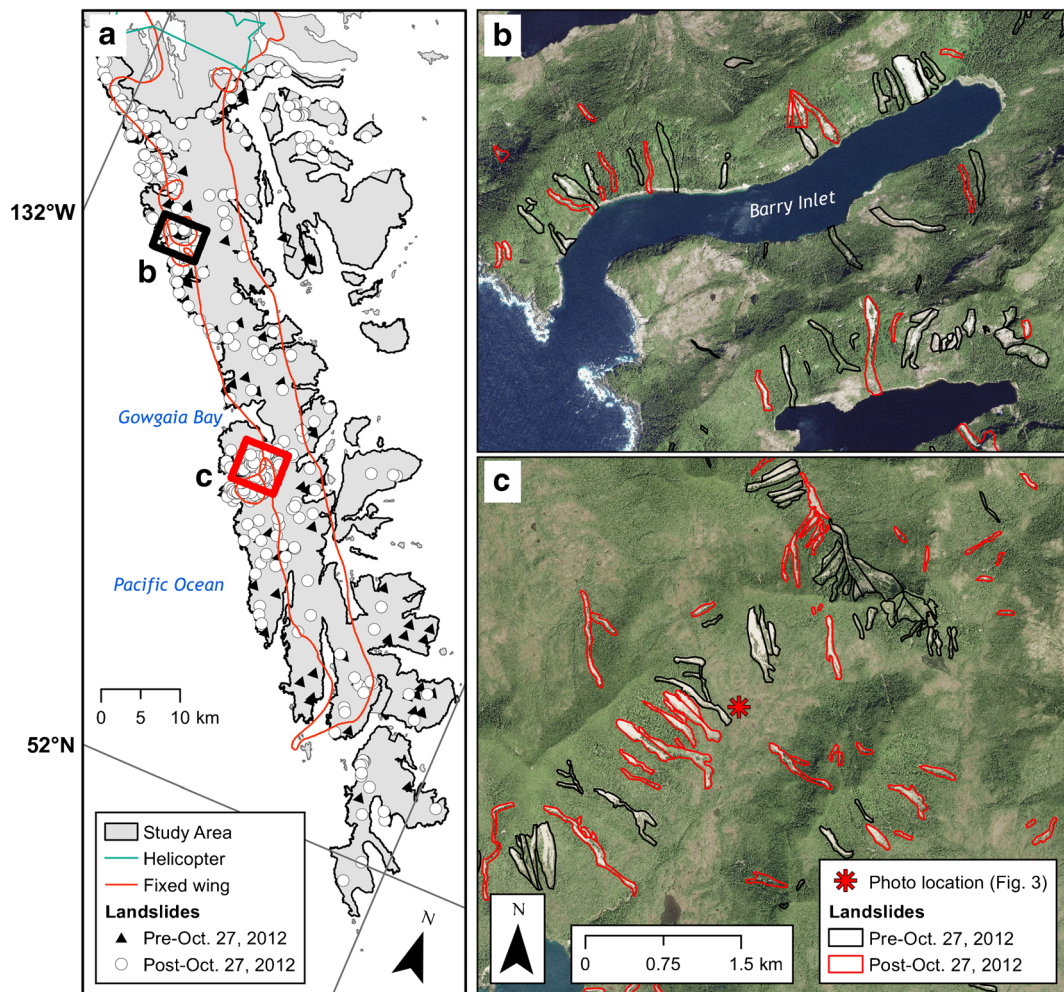


**Fig. 4** a Map showing aerial reconnaissance flight track and locations of pre- and post-earthquake landslides. b, c Inset images (locations shown in a), providing details of pre- and post-earthquake landslides overlain on 2017 summer SPOT 6/7 satellite imagery

the study area, whereas the earlier flight was at the north end of the area. The two flights constrain the time of fresh landslides to shortly after the earthquake, but before the first cloud-free satellite images were acquired. We photographed all landslides that we saw during the reconnaissance flights and recorded their locations on the flight GPS tracks.

### Aerial and satellite imagery

We created landslide polygons by interpreting 2007 aerial photographs and high-resolution RapidEye and PlanetScope satellite images (Table 1). The 2007 air photos are the most recent pre-earthquake air photos. Satellite imagery also exists; however, the air photos offer a much higher spatial resolution (25 cm; Table 1). We also used cloud-free satellite images from 2012, 2013, and 2016 acquired by the RapidEye (5 m resolution) satellite constellation and from 2018 acquired by the PlanetScope Dove (3 m resolution) constellation (Planet Team 2017). Both include visible and near-infrared spectral bands that assist in landscape interpretation.

### Landslide mapping

We manually digitized landslide polygons from the available imagery listed in Table 1. We assume that no mapped landslide in the earliest image (2007) experiences a full ecological recovery in the subsequent imagery. Smith et al. (1986) observed that landslides on upper slopes of volcanic bedrock on Haida Gwaii require 40 years to become about 50% revegetated, although revegetation would be more rapid on lower slope positions and on other substrates.

The imagery we used to determine average annual landslide rates and distribution in the study area over a period of almost 11 years is limited by several factors, including cloud cover, snow, shadows, and image resolution. Frequent cloud cover led to the exclusion of some images. In a few instances, we had to use coarser satellite images to patch holes in our imagery and complete the inventory. Although snow on Haida Gwaii tends to accumulate only at high elevations, above where most landslides occur, it is possible that some landslides were hidden by snow. Furthermore, shadows on steep mountainous slopes and the forest canopy can obscure small landslides. Due to the spatial resolution of the post-earthquake imagery, the detection of small landslides was challenging.

We delimited landslide polygons on the 2013 imagery and examined older images to detect landslides older than the 2012 earthquake. To obtain a better understanding of the frequency of

landslides after the earthquake, we extended the inventory to 2018 and drew polygons on the 2016 and 2018 images. We mapped individual landslides and landslide complexes. We classified landslides with one headscarp, but two or more slide paths as single landslides. Landslides with several distinct headscarps and slide paths that coalesced were counted as multiple landslides. We summed and averaged the number and area of these polygons to determine the normalized yearly number and size of the landslides from 2007 to 2018. We categorized all landslides that happened within the decade by type using the nomenclature of Cruden and Varnes (1996).

## Results

### Landslide inventory

We identified and mapped 446 landslide polygons in our 1350 km<sup>2</sup> study area; 95% were classified as debris slides (e.g. Fig. 3) and 5% as debris flows. The areas of the smallest, the average, and the largest detected landslide were 0.089, 1.9, and 24.3 ha, respectively. Millard et al. (2012) observed a few rockslides north of our study, but we found none in our study area. Many of the landslides initiated in Folsols directly below hill crests.

### Landslide time series

The graphs in Fig. 5 show landslide numbers and total area in relation to the year in which the landslides first appeared. We normalized the number of observed landslides and their total area by the number of years separating the five different data acquisitions.

We mapped 97 landslides for the pre-earthquake period (2007–2012), yielding an annual rate of 1.44 landslides per 100 km<sup>2</sup>/year, which represents 19.4 landslides per year (Fig. 5a). The total annual landslide area for that period is 0.35 km<sup>2</sup> (35 ha, Fig. 5b), with an average pre-earthquake landslide area of 0.36 ha (total area/count) for this period.

We mapped 244 landslides between September 2012 (pre-earthquake) and May 2013 (post-earthquake). We consider them to be seismically induced, probably co-seismic, landslides based on observations made during our overview flights (Fig. 4) and eyewitness accounts on northern Haida Gwaii (Millard et al. 2012). The calculated frequency of post-earthquake landslides is 18.1 landslides per 100 km<sup>2</sup>/year, representing a 12.9-fold increase over the previous annual landslide rate and a 65.8-fold increase in

**Table 1** Aerial and satellite imagery used in the landslide inventory (BW black and white; VIS red, green, and blue; NIR near infrared)

Acquisition (YYYY-MM-DD)	Sensor/platform	Resolution	Spectral bands	Data source
2007-09 2007-08	Air photo	25 cm	BW	Province of British Columbia (2018)
2012-07-15 2012-07-16 2012-09-06 2012-09-18	RapidEye-3 RapidEye-4 RapidEye-3 RapidEye-1	5 m	VIS + NIR	Planet Team (2017)
2013-05-05 2013-07-28	RapidEye-1 RapidEye-5	5 m	VIS + NIR	Planet Team (2017)
2016-05-11 2016-05-12	RapidEye-4 RapidEye-5	5 m	VIS + NIR	Planet Team (2017)
2018-10-13	PlanetScope	3 m	VIS + NIR	Planet Team (2017)

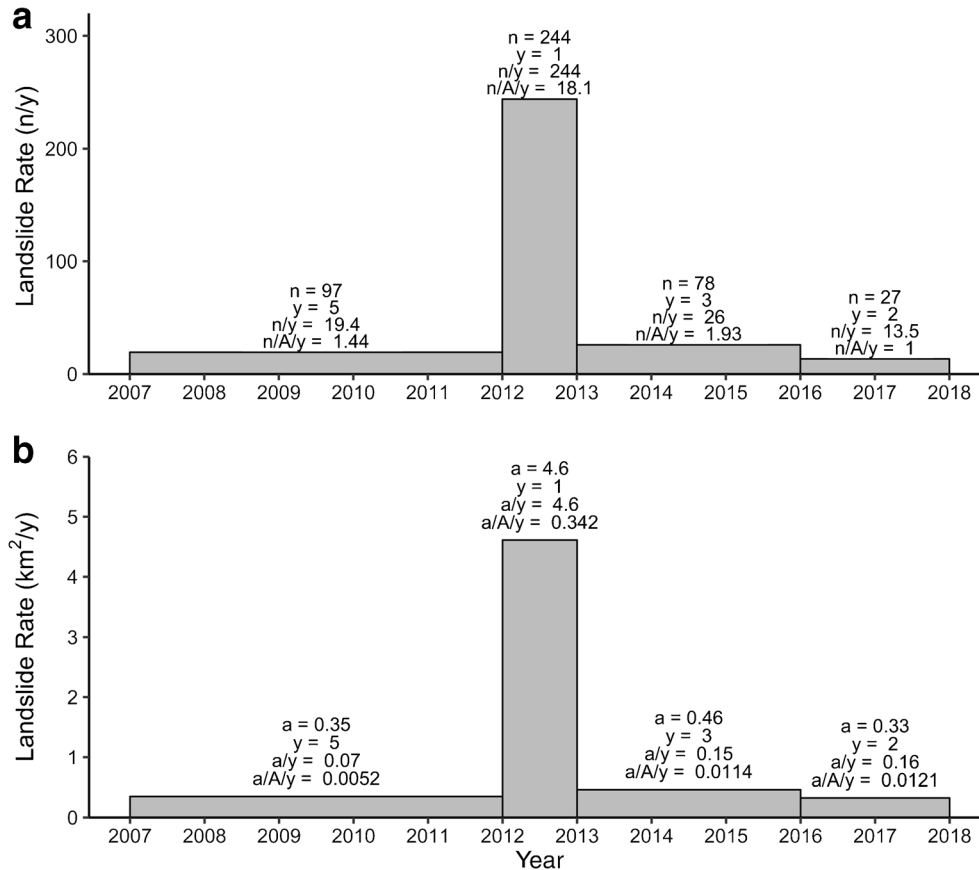


**Fig. 5** a Landslide counts over time ( $n$  = number,  $y$  = years,  $n/y$  = number per year). b Total landslide area over time ( $a$  = area in  $\text{km}^2$ ,  $y$  = years,  $a/y$  = area in  $\text{km}^2$  per year)

annual landslide area per 100  $\text{km}^2/\text{year}$  (Fig. 5). Average landslide size increased from 0.36 ha to 1.88 ha.

After this spike, the rates and numbers of landslides decreased. In the next three years (2013–2016), we identified an additional 78 landslides, and in the following two years (2016–2018), we recognized another 27 landslides (Fig. 5a). Between May 2013 and May 2016, we identified an average of 26 landslides per year, and between 2016 and 2018, the number decreased further to 13.5 landslides per year (Fig. 5a). Annual landslide rates per 100  $\text{km}^2$  are, respectively, 1.93 and 1.0 for the two periods (Fig. 5a). The average size of the post-earthquake landslides, however, is lower for the 2013–2016 period (0.59 ha) than for the 2016–2018 period (1.22 ha).

#### Aspect

Figure 6 shows the percentage area covered by landslides in relation to their slope aspects (normalized to available slopes). The plot on the left shows the aspects of landslides prior to the earthquake; the middle plot shows aspects of inferred earthquake-induced landslides; and the plot on the right shows aspects of landslides that happened after the earthquake (2013–2018), a period during which there were no major earthquakes.

Prior to 2012, most of the area covered by landslides occurred on slopes facing west (14%), southwest (20%), and south (25%) (Fig. 6), whereas 11%, 7%, and 11% occurred on, respectively,

northwest-, north-, and northeast-facing slopes, and only 6% and 7% occurred on east and southeast facing slopes (Fig. 6). In contrast up to 20%, 17%, and 12% of landslides in 2012–2013 occurred on northwest-, north-, and southeast-facing slopes (Fig. 6). In the 6 years following the earthquake, only 6.8% of landslide area occurred on northwest-facing slopes, and the slope aspect distribution resembles the pre-earthquake conditions (Fig. 6).

#### Rainfall analysis

The Sandspit A climate station (Fig. 1) experienced 49 mm of precipitation on 15 October 2012, a few days before the earthquake. Precipitation recorded during the months following the earthquake was normal, and precipitation during November of that year was 31 mm, near the average value (Fig. 8). The Cape St James station recorded 66 mm of rainfall on 22 February 2013, 4 months after the earthquake (Fig. 8), but some precipitation data for this station in the months following the earthquake are missing.

On 4 November 2012, a storm with southwest winds up to 120 km/h was recorded at Cape St. James. On the same day, southeast winds with a maximum speed of 124 km/h were measured at the Cumshewa weather station north of Gwaii Haanas. One day earlier, even higher southerly gusts of 139 km/h were recorded at the Cumshewa station.

Storms with heavy rainfall occur frequently on the west coast of Haida Gwaii. The Cumshewa Island station recorded several

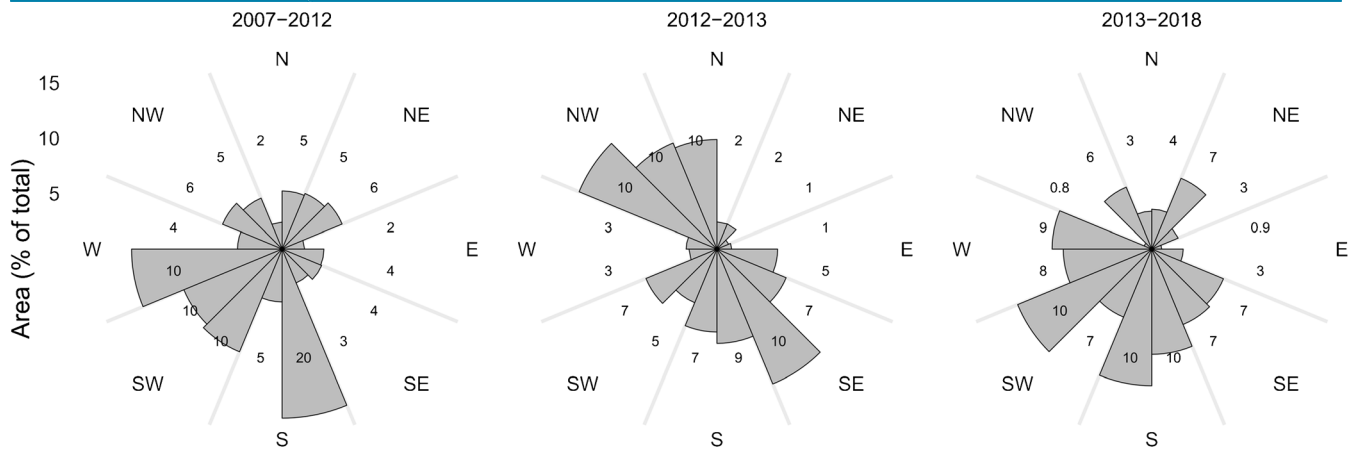


**Fig. 6** Rose diagrams of slope aspects of landslides that occurred over different periods. The area (percentage of total) is labelled on each diagram for each bar at the 10% line, and these values have been rounded and may not add up to 100%. Note the much greater percentage of landslide area on north- and northwest-facing slopes in the centre plot, which is the group of landslides associated with the earthquake

severe storms during the period of this study. For example, storms with maximum wind gust speeds of 130 km/h and 128 km/h occurred, respectively, in March 2008 and December 2015. In one day in January 2016, 74 mm of rain fell at the Cumshewa Island weather station, and in October 2009 nearly 80 mm of rain fell at that station within 24 h.

## Discussion

### Earthquake-induced landslide spike

There was a notable spike in landslides after the 2012 Haida Gwaii earthquake. Of the 446 landslides that we identified between 2007 and 2018, 244 were seismically induced and probably co-seismic. More than 100 were validated during reconnaissance flights in 2012, less than 2 weeks after the earthquake, along with some eyewitness accounts of co-seismic landslides north of the study area (Millard et al. 2012).

The spike in landslides triggered by the earthquake represents a 12.9-fold increase in the number of landslides over the background rate (Fig. 5). The same dataset expressed in terms of area yields a 65.8-fold increase in landslide area, from 0.07 km<sup>2</sup>/year to 4.6 km<sup>2</sup>/year. The average area of the 244 seismically induced landslides is 1.88 ha, which is about five times higher than the area of landslides prior to the earthquake.

There were no significant storms or periods of heavy rainfall at the time of, or shortly after, the earthquake that might account for the spike in landslides. This fact increases the significance and likelihood of them being earthquake-triggered.

Earthquake-induced landslide spikes have been reported in many regions of the world, although not associated with shallow Folisols. Our data show that shallow organic Folisols on Canada's west coast are susceptible to failure during strong earthquakes.

### 7.2 Landslide locations

The nearest seismometer to the study area (Barry Inlet on the west coast of Moresby Island) was damaged by the earthquake.

The remaining weak-motion seismometers on Haida Gwaii were saturated by the strong shaking. Strong motion Internet Accelerometers (IAs), however, recorded the earthquake well and indicated a peak horizontal acceleration of 0.2 g at the Village of Queen Charlotte, 80 km from the epicentre (Rosenberger et al. 2013). Ground accelerations within Gwaii Haanas Park would have exceeded 0.2 g ( $\sim 1.96 \text{ m/s}^2$ ), based on the ground motion equations of Atkinson and Adams (2013), which most closely match Peak Ground Accelerations (PGA) measured at the three IAs. We note that people on Haida Gwaii reported very strong shaking (at Modified Mercalli Intensity VII) more than 150 km from the epicentre.

Non-seismic landslides that happened before the earthquake were concentrated on south and southeast slopes, which face the prevailing storms and winds (Figs. 6 and 7). In contrast, most of the earthquake-induced landslides face northwest. The Centroid Moment Tensor solution for the earthquake (Kao et al. 2015) indicates thrust displacements to the northeast, which would cause the overriding crust to shift to the southwest. GPS measurements by Nykolaishen et al. (2015) verify the conclusion of Kao et al. (2015) and show that Moresby Island moved as much as 1.15 m to the southeast and subsided by as much as 0.3 m during the earthquake. This movement may have produced instantaneous increases in pore pressure in water-saturated Folisols on the north-facing slopes that historically experience less failure.

Numerous previous studies have contrasted seismic from rain-induced landslides (Tibaldi et al. 1995; Okushi et al. 1999; Chang et al. 2007; Wang et al. 2007; Lin et al. 2008; Meunier et al. 2008; Qi et al. 2010; Gorum et al. 2011). Earthquake-induced landslides have affinities to faults and ridge crests, and in some cases to particular geological units. In contrast, rain-induced landslides commonly occur on lower slopes (Chang et al. 2007). In our study, both rain- and seismically induced landslides initiated on upper slopes near ridge crests. This strong association with ridge crests may have something to do with the low strength of organic Folisols, which occupy these upper slopes (Banner et al. 2014).

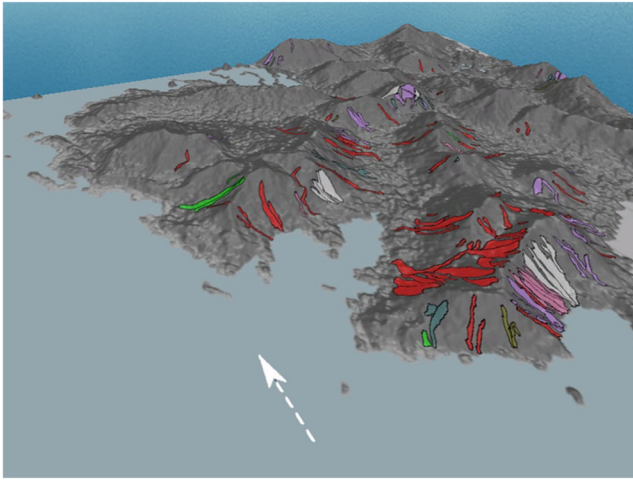


**Fig. 7** Oblique view of Haida Gwaii landslides just south of Gowaia Bay (see Fig. 4 for location). For the entire study area some 39% of the earthquake-induced landslide area (red) occurred on north-facing slopes, in the lee of prevailing weather systems. In comparison, less than 34% of the area of pre-earthquake, non-seismic landslides (white pre 1952, purple pre 1984, pink pre 1994, yellow pre 2007, green 2012) occurs on north-facing slopes. North arrow (white dashed line) is 2 km long

Fewer studies have noted aspect relationships of earthquake-induced landslides (Mathews 1979, Tibaldi et al. 1995; Okushi et al. 2019; Chang et al. 2007). The main difference between our dataset and those of previous researchers is that many of our earthquake-induced landslides (37% N-NW slopes) occurred on slopes with different aspects than those of rain-induced landslides (18% N-NW slopes) (Figs. 6 and 7).

Mathews (1979, Canada), Tibaldi et al. (1995; Ecuador), Okunishi et al. (1999; Japan), and Wang et al. (2007; Taiwan) found that co-seismically triggered landslides tended to occur on slopes facing away from the earthquake epicentre. In contrast, a disproportionately large number of the co-seismic Haida Gwaii landslides occurred on slopes facing the epicentre. This may have more to do with the earthquake's rupture mechanism influencing directivity of ground motion and hence affected slope aspects than simple epicentral direction.

### Conclusion

We document an order-of-magnitude increase in the number of debris slides and debris flows during and shortly after the Haida Gwaii earthquake of 27 October 2012. The number of landslides increased 12.9 times and the area of landslides increased 65.8 times immediately after the earthquake. Average landslide area increased from 0.07 km<sup>2</sup> per year to 4.6 km<sup>2</sup> per year, and the average size of landslides increased from 0.36 ha/year immediately before the earthquake to 1.88 ha/year afterwards. Landslide rates and sizes returned to near pre-2012 levels in the years after the earthquake, although they remained slightly elevated.

Most non-seismically triggered landslides in our study area occur on south- and southwest-facing slopes in the direction of the prevailing winds and storms. In contrast, some 32% of the seismically induced landslides occurred on north- and northwest-facing slopes, and 33% on south- and southeast-facing slopes in the direction of the earthquake epicentre. This contrasts with other studies that have shown a preference for landslides to face away from earthquake epicentres. This may relate to the earthquake's rupture mechanism influencing directivity of ground motion.

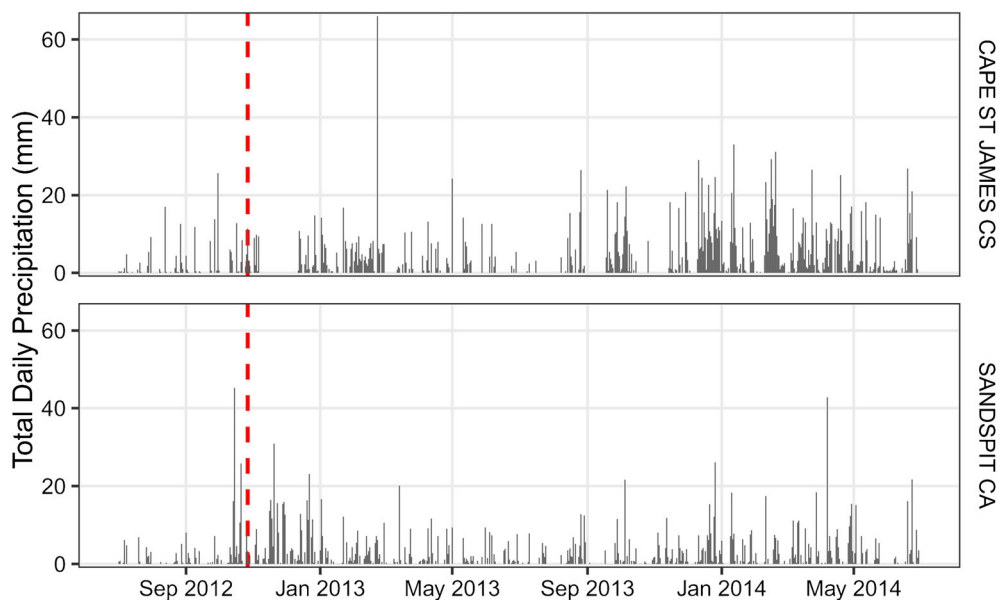


**Fig. 8** Top: Daily precipitation from 1 July 2012 to 1 December 2013 at the Cape St. James weather station. Bottom: Daily precipitation from 1 July 2012 at Sandspit A weather station. Dashed red lines represent the timing of the 27-10-2012 earthquake. See Figure 1 for locations of weather stations



## Acknowledgements

We thank Planet Labs for access to their imagery database.

**Open Access** This article is distributed under the terms of the Creative Commons Attribution 4.0 International License (<http://creativecommons.org/licenses/by/4.0/>), which permits unrestricted use, distribution, and reproduction in any medium, provided you give appropriate credit to the original author(s) and the source, provide a link to the Creative Commons license, and indicate if changes were made.

## References

- Atkinson GM, Adams J (2013) Ground motion prediction equations for application to the 2015 Canadian national seismic hazard maps. *Can J Civ Eng* 40:988–998. <https://doi.org/10.1139/cjce-2012-0544>
- Banner A, MacKenzie WH, Pojar J, MacKinnon A, Saunders SC, Klassen H (2014) A field guide to ecosystem classification and identification for Haida Gwaii. *Prov BC Land Manag Handb* 68 [www.for.gov.bc.ca/hfd/pubs/Docs/Lmh/Lmh68.htm](http://www.for.gov.bc.ca/hfd/pubs/Docs/Lmh/Lmh68.htm)
- Bevington A, Clague JJ, Millard T, Walker IJ, Geertsema M (2017) The diverse landscapes of Haida Gwaii. In: Slaymaker O (ed), *Landscapes and Landforms of Western Canada*. Springer Intern Publ 291–302. [https://doi.org/10.1007/978-3-319-44595-3\\_21](https://doi.org/10.1007/978-3-319-44595-3_21)
- Bird AL, Lamontagne M (2015) Impacts of the October 2012 magnitude 7.8 earthquake near Haida Gwaii, Canada. *Bull Seismol Soc Am* 105(2B):1178–1192. <https://doi.org/10.1785/0120140167>
- Blais-Stevens A, Maynard D, Weiland I, Geertsema M, Behnia P (2016) Surficial geology and landslide inventory in Douglas Channel fjord, northwest British Columbia. *Proc GeoVancouver, Vancouver*
- Bostwick TK (1984) A Re-examination of the August 22, 1949 Queen Charlotte Earthquake. Univ BC, Vancouver, BC. PhD Thesis <https://doi.org/10.14288/1.0052501>
- Cassidy JF, Rogers GC, Hyndman RD (2014) An overview of the 28 October 2012  $M_w$  7.7 earthquake in Haida Gwaii, Canada: A tsunamigenic thrust event along a predominantly strike-slip margin. *Pure Appl Geophys* 171:3457–3465. <https://doi.org/10.1007/s00024-014-0775-1>
- Chang K-T, Chiang S-H, Hsu M-L (2007) Modeling typhoon- and earthquake-induced landslides in a mountainous watershed using logistic regression. *Geomorphology* 89:335–347
- Cloutier C, Locat J, Geertsema M, Jakob M, Schnorbus M (2016) Potential impacts of climate change on landslide occurrence in Canada. In: Ho KKS, Lacasse S, Picarelli L (eds) *Slope Safety Preparedness for Impact of Climate Change*. CRC, Boca Raton, pp 71–104. <https://doi.org/10.1201/9781315387789-3>
- Cruden DM, Varnes DJ (1996) Landslide types and processes. In: Turner AK, Shuster, RL (eds), *Landslides Investigation and Mitigation*. Nat Res Council, Transport Res Bd, Spec Rep 247: 36–75
- DeMets C, Gordon RG, Argus DF, Stein S (1990) Current plate motions. *Geophys J Int* 101(2):425–478. <https://doi.org/10.1111/j.1365-246X.1990.tb06579.x>
- Evans SG, Clague JJ (1994) Recent climatic change and catastrophic geomorphic processes in mountain environments. *Geomorphology* 10:107–128. [https://doi.org/10.1016/0169-555X\(94\)90011-6](https://doi.org/10.1016/0169-555X(94)90011-6)
- Fox CA, Tarnocai F (2011) Organic soils of Canada. Part 2. Upland organic soils. *Can J Soil Sci* 91(5):823–842. <https://doi.org/10.4141/cjss10032>
- Geertsema M, Pojar JJ (2007) Influence of landslides on biophysical diversity – a perspective from British Columbia. *Geomorphology*. 89:55–69. <https://doi.org/10.1016/j.geomorph.2006.07.019>
- Geertsema M, Clague JJ, Schwab JW, Evans SG (2006) An overview of recent large catastrophic landslides in northern British Columbia, Canada. *Eng Geol* 83:120–143. <https://doi.org/10.1016/j.enggeo.2005.06.028>
- Geertsema M, Highland LM, Vauegois L (2009) Environmental impact of landslides. In: Sassa K, Canuti P (eds) *Landslides – Disaster Risk Reduction*. Springer-Verlag, Berlin Heidelberg, pp 585–607. [https://doi.org/10.1007/978-3-540-69970-5\\_31](https://doi.org/10.1007/978-3-540-69970-5_31)
- Gimbarzevsky P (1988) Mass wasting on the Queen Charlotte Islands: a regional inventory. *Prov BC Land Manag Rep* 29. <https://www.for.gov.bc.ca/hfd/pubs/Docs/Mr/Lmr029.htm>
- Gorum T, Fan X, van Westen CJ, Huang RQ, Xu Q, Tang C, Wang G (2011) Distribution pattern of earthquake-induced landslides triggered by the 12 May 2008 Wenchuan earthquake. *Geomorphology* 133:152–167
- Guthrie RH, Evans SG (2004) Analysis of landslide frequencies and characteristics in a natural system, coastal British Columbia. *Earth Surf Process Landf* 29:1321–1339. <https://doi.org/10.1002/esp.1095>
- Jagiello L, Martin YE, Sjogren DB (2012) Scaling and multivariate analysis of medium to large landslide events: Haida Gwaii, British Columbia. *Nat Hazards* 60:321–344. <https://doi.org/10.1007/s11069-011-0012-5>
- Jakob M (2000) The impacts of logging on landslide activity at Clayoquot Sound, British Columbia. *Catena* 38:279–300. [https://doi.org/10.1016/S0341-8162\(99\)00078-8](https://doi.org/10.1016/S0341-8162(99)00078-8)
- Jakob M, Lambert S (2009) Climate change effects on landslides along the southwest coast of British Columbia. *Geomorphology* 107:275–284. <https://doi.org/10.1016/j.geomorph.2008.12.009>
- Jibson RW, Harp EL, Schulz W, Keefer DK (2006) Large rock avalanches triggered by the M 7.9 Denali Fault, Alaska, earthquake of 3 November 2002. *Eng Geol* 83:144–160. <https://doi.org/10.1016/j.enggeo.2005.06.029>
- Kao H, Shan S-J, Farahbod AM (2015) Source characteristics of the 2012 Haida Gwaii earthquake sequence. *Bull Seismol Soc Am* 105:1206–1218. <https://doi.org/10.1785/0120140165>
- Kargel JS, Leonard GJ, Shugar DH, Haritashya UK, Bevington A et al (2016) Geomorphic and geologic controls of geohazards induced by Nepal's 2015 Gorkha earthquake. *Science* 351:aac8353. <https://doi.org/10.1126/science.aac8353>
- Keefer DK (2000) Statistical analysis of an earthquake-induced landslide distribution—The 1989 Loma Prieta, California event. *Eng Geol* 58:231–249. [https://doi.org/10.1016/S0013-7952\(00\)00037-5](https://doi.org/10.1016/S0013-7952(00)00037-5)
- Krag RK, Sauder EA, Wellburn GV (1986) Forest engineering analysis of landslides in logged areas on the Queen Charlotte Islands, British Columbia. *Prov BC Land Manag Rep* 43. <https://www.for.gov.bc.ca/hfd/pubs/Docs/Mr/Lmr043.htm>
- Lin C-W, Liu S-H, Lee S-Y, Liu C-C (2006) Impacts of the Chi-Chi earthquake on subsequent rainfall-induced landslides in central Taiwan. *Eng Geol* 86:87–101. <https://doi.org/10.1016/j.enggeo.2006.02.010>
- Lin G-W, Chen H, Hovius N, Horng M-J, Dadson S, Meunier P, Lines M (2008) Effects of earthquake and cyclone sequencing on landsliding and fluvial sediment transfer in a mountain catchment. *Earth Surf Process Landf* 33:1354–1373
- Martin Y, Rood K, Schwab JW, Church M (2002) Sediment transfer by shallow landsliding in the Queen Charlotte Islands, British Columbia. *Can J Earth Sci* 39:189–205. <https://doi.org/10.1139/e01-068>
- Mathews WH (1979) Landslides of central Vancouver Island and the 1946 earthquake. *Bull Seismol Soc Am* 69:445–450
- Meunier P, Hovius N, Haines JA (2008) Topographic site effects and the location of earthquake induced landslides. *Earth Planet Sci Lett* 275:221–232
- Millard T, Geertsema M, Clague J, Bobrowsky P, Sakals M (2012) Landslides on Haida Gwaii during and after the earthquake. *Risky Ground, Winter 2012*: 12–13. [http://www.sfu.ca/cnr/news\\_events/newsletter/RiskyGround\\_News\\_2012-12-21.pdf](http://www.sfu.ca/cnr/news_events/newsletter/RiskyGround_News_2012-12-21.pdf)
- Nagle HK (2000) Follic debris slides near Prince Rupert, British Columbia. MSc thesis, Univ Alberta, Edmonton, AB, 189 pp
- Nykolaishen L, Dragert H, Wang K, James TS, Schmidt M (2015) GPS observations of crustal deformation associated with the 2012  $M_w$  7.8 Haida Gwaii earthquake. *Bull Seismol Soc Am* 105(2B):1241–1252. <https://doi.org/10.1785/0120140177>
- Okunishi K, Sonoda M, Yokoyama K (1999) Geomorphic and environmental controls of earthquake-induced landslides. *Trans Japan Geomorph Un* 20:351–368
- Planet Team (2017) Planet Application Program interface: In: *Space for Life on Earth*. San Francisco. <https://api.planet.com>
- Poulin VA (1984) A Research Approach to Solving Fish/Forestry Interaction in Relation to Mass Wasting on the Queen Charlotte Islands. *Prov BC Land Manag Rep* 27. <https://www.for.gov.bc.ca/hfd/pubs/Docs/Mr/Lmr027.htm>
- Province of British Columbia (2018) Haida Gwaii air photos, 1:20:000: BCC07069 (1-158); BCC07070 (1-108); BCC07071 (1-215). Prov BC, Victoria
- Qi S, Xu Q, Lan H, Zhang B, Liu J (2010) Spatial distribution of landslides triggered by 2008.5.12 Wenchuan earthquake, China. *Eng Geol* 116:95–108
- Rollerson TP (1992) Relationships between landscape attributes and landslide frequencies after logging: Skidegate Plateau, Queen Charlotte Islands. *Prov BC, Land Manag Rep* 76. <https://www.for.gov.bc.ca/hfd/pubs/Docs/Mr/Lmr076.htm>
- Rood KM (1984) An Aerial Photograph Inventory of the Frequency and Yield of Mass Wasting on the Queen Charlotte Islands, British Columbia. *Prov BC, Land Manag Rep* 34. <https://www.for.gov.bc.ca/hfd/pubs/Docs/Mr/Lmr034.htm>
- Rood KM (1990) Site Characteristics and landsliding in forested and clearcut terrain, Queen Charlotte Islands, B.C. *Prov BC, Land Manag Rep* 64. <https://www.for.gov.bc.ca/hfd/pubs/Docs/Mr/Lmr064.htm>
- Rosenberger A, Bird A, Turek ME, Huffman S, Rogers G, Cassidy J, Mulder T (2013) Strong motion data from the magnitude 7.7 “Haida Gwaii” Earthquake on October 27, 2012 (Local Time). *Geol Surv Can, Open File* 7324, 34 pp. <https://doi.org/10.4095/292275>

- Schuster RL, Highland LM (2007) Overview of the effects of mass wasting on the natural environment. *Environ Eng Geosci* 13:25–44. <https://doi.org/10.2113/gseegeosci.13.1.25>
- Schwab JW (1983) Mass Wasting, October–November 1978 Storm, Rennell Sound, Queen Charlotte Islands, British Columbia. *Prov BC Res Note* 91. <https://www.for.gov.bc.ca/hfd/pubs/Docs/Mr/Scanned-Rn/Rn067-Rn100/Rn091.pdf>
- Schwab JW (1988) Mass wasting impacts to forest land: forest management implications, Queen Charlotte Islands, Queen Charlotte Timber Supply Area. In: Lousier, JD, Still, GW (eds), *Degradation of Forest Land: Forest Soils at Risk*. Proc 10th BC Soil Sci Workshop Feb 1986. BC Min Forests, Land Management Rep 56, pp 104–115. [www.for.gov.bc.ca/hfd/pubs/Docs/Mr/Lmr/Lmr056.pdf](http://www.for.gov.bc.ca/hfd/pubs/Docs/Mr/Lmr/Lmr056.pdf)
- Schwab JW (1998) Landslides on the Queen Charlotte Islands: Processes, rates and climatic events. In: Hogan DL, Tschaplinski PJ, Chatwin S (eds), *Carnation Creek and Queen Charlotte Islands Fish/Forestry Workshop: Applying 20 Years of Coast Research to Management Solutions*. *Prov BC Land Manag Handb* 41. <https://www.for.gov.bc.ca/hfd/pubs/docs/Lmh/LMH41-1.pdf>
- Septer D, Schwab JW (1995) Rainstorm and flood damage, Northwest British Columbia 1891–1991. *Prov BC Land Manag Handb* 31. <https://www.for.gov.bc.ca/hfd/pubs/docs/Lmh/Lmh31.pdf>
- Smith RB, Commandeur PR, Ryan MW (1986) Soils, vegetation, and forest growth on landslides and surrounding logged and old-growth areas on the Queen Charlotte Islands. *Prov BC Land Manag Rep* 41. <https://www.for.gov.bc.ca/hfd/pubs/Docs/Mr/Lmr/Lmr041.pdf>
- Soil Classification Working Group (1998) The Canadian system of soil classification (3rd ed). *Agri Agri-Food Can, Nat Res Counc Press Publ* 646. [http://sis.agr.gc.ca/cansis/publications/manuals/1998-css-ed3/css3\\_manual.pdf](http://sis.agr.gc.ca/cansis/publications/manuals/1998-css-ed3/css3_manual.pdf)
- Sutherland Brown A (1968) Geology of the Queen Charlotte Islands British Columbia. BC Dep Mines Petrol Resourc Bull 54, 226 pp. [http://cmscontent.nrs.gov.bc.ca/geoscience/PublicationCatalogue/Bulletin/BCGS\\_B054.pdf](http://cmscontent.nrs.gov.bc.ca/geoscience/PublicationCatalogue/Bulletin/BCGS_B054.pdf)
- Tanyaş H, Van Westen CJ, Allstadt KE et al (2017) Presentation and analysis of a worldwide database of earthquake-induced landslide inventories. *J Geophys Res Earth Surf* 122:1991–2015. <https://doi.org/10.1002/2017JF004236>
- Tibaldi A, Ferrari L, Pasquare G (1995) Landslides triggered by earthquakes and their relations with faults and mountain slope geometry: An example from Ecuador. *Geomorphology* 11:215–226
- Tschaplinski PJ, Hogan D, Hartman GF (2004) Fish-forestry interaction research in coastal British Columbia: The Carnation Creek and Queen Charlotte Islands studies. In: Northcote TG, Hartman GF (eds) *Fishes Forestry: Worldwide Watershed Interactions Manage*. Blackwell Science Ltd, Oxford. <https://doi.org/10.1002/9780470995242.ch18>
- Vittoz P, Stewart GH, Duncan RP (2001) Earthquake impacts in old-growth *Nothofagus* forests in New Zealand. *J Veg Sci* 12:417–426. <https://doi.org/10.2307/3236856>
- Wang H, Sassa K (2006) Analysis of seismically triggered landslides in the 2004 Chuetsu event of Niigata prefecture, Japan. IAEG2006 Paper number 174, 9 pp
- Wang HB, Sassa K, Xu WY (2007) Analysis of a spatial distribution of landslides triggered by the 2004 Chuetsu earthquakes of Niigata Prefecture, Japan. *Nat Hazards* 41:43–60. <https://doi.org/10.1007/s11069-006-9009-x>
- Wang T, Hamann A, Spittlehouse DL, Murdock TQ (2012) Climate WNA-high-resolution spatial climate data for western North America. *J Appl Meteorol Climatol* 51:6–29. <https://doi.org/10.1175/JAMC-D-11-043.1>
- Wells A, Duncan RP, Stewart GH (2001) Forest dynamics in Westland, New Zealand: The importance of large, infrequent earthquake-induced disturbance. *J Ecol* 89:1006–1018. <https://doi.org/10.1111/j.1365-2745.2001.00594.x>
- Xu C, Xu X, Yao X, Dai F (2014) Three (nearly) complete inventories of landslides triggered by the May 12, 2008 Wenchuan  $M_w$  7.9 earthquake of China and their spatial distribution statistical analysis. *Landslides* 11:441–461. <https://doi.org/10.1007/s10346-013-0404-6>
- Yin Y, Wang F, Sun P (2009) Landslide hazards triggered by the 2008 Wenchuan earthquake, Sichuan, China. *Landslides* 6:139–152. <https://doi.org/10.1007/s10346-009-0148-5>

**S. Barth · M. Geertsema · A. R. Bevington · T. Millard**

British Columbia Ministry of Forests, Lands, Natural Resource Operations, and Rural Development,  
Prince George, BC V2L 1R5, Canada

**S. Barth**

Universität Potsdam,  
14476, Golm, Potsdam, Germany

**M. Geertsema** (✉) · **A. R. Bevington**

Natural Resources and Environmental Studies Institute and Geography Program,  
University of Northern British Columbia,  
Prince George, BC V2N 4Z9, Canada  
Email: Marten.Geertsema@gov.bc.ca

**A. L. Bird · P. T. Bobrowsky**

Geological Survey of Canada,  
Sidney, BC V8L 4B2, Canada

**J. J. Clague**

Department of Earth Sciences,  
Simon Fraser University,  
Burnaby, BC V5A 1S6, Canada

**A. Hasler**

SensAlpin,  
promenades 129, CH-7260, Davos Dorf, Switzerland

**H. Liu**

Yunnan University of Finance and Economics,  
2502 Gaodeng St, Chenggong Qu, Kunming Shi, 650503, Yunnan Sheng, China